Chapter 1

Fourier Transform Infrared and Raman Characterization of Silica-Based Materials

Larissa Brentano Capeletti and
João Henrique Zimnoch

Additional information is available at the end of the chapter

http://dx.doi.org/10.5772/64477

Abstract

Fourier Transform Infrared and Raman are powerful techniques to evaluate silica and hybrid silica structure. It is possible to evaluate the silica network formation along the hydrolysis and condensation reactions in terms of siloxane rings formation and Si–O(–Si) angle deformation due to the introduction of organic groups, the employed synthetic route or encapsulated species interaction. The siloxane four- or six-membered rings imply in a more rigid or flexible network, respectively, in order to accommodate the organic groups. A structural analysis of the materials is of high importance, since interactions between the encapsulated molecules and the matrix are critical for the device performance, such as sensors. This type of device needs the permeation of an analyte to activate the encapsulated receptor molecules inside the silica structure. Fourier transform infrared spectrometry can be also used to determine parameters of the silica network as a function of the hydrophilicity/hydrophobicity degree and the siloxane ring structure with respect to thin film porosity. This silica structural analysis is reviewed along the text in a tentative of better exploring the data resulting from these powerful techniques. In addition, the functionalization of silica structures by the use of organoalkoxysilanes, which is important to the creation of high-specific materials, can be well described by these two complementary techniques. The Si–C bonds and the maintenance of the organic substituents such as methyl, octyl, octadecyl, vinyl, phenyl, aminopropyl, mercaptopropyl, isocyanatopropyl, iodopropyl, chloropropyl and glicydoxypropyl could be evaluated after the sol-gel synthesis process. The literature regarding silica vibrational spectroscopy is also explored creating a data bank of wave numbers for the most important bonds for different types of silica and hybrid silica materials obtained by different synthetic routes.

Keywords: hybrid silica, molecular imprinting, silica-based materials, FTIR, Raman

1. Introduction on silica-based materials

Silica-based materials have a wide field of applications nowadays, since it is very flexible in terms of material characteristics and fabrication methods [1]. Different types of devices such as catalysts, chromatographic phases, sorbents, sensors, coatings, etc. can be produced with tuned properties to enhance activity and/or robustness.

In terms of catalysts, several different reactions can take advantage of the silica surface usage, resulting in heterogeneous processes. The hydrogen production, for example, needs high surface area supports, open porosity, nanostructure with uniform morphology, highly and relatively uniform dispersed active phase, which can be achieved by a silica matrix [2]. In addition, very complex structures can be designed as rattle-type magnetic silica composite with nonporous silica-coating magnetic iron oxide encapsulated in mesoporous silica hollow sphere which can also contain active metallic nanoparticles (**Figure 1A**), resulting in a Pt-based catalyst for hydrogenation that exhibits high activity, selectivity and excellent reusability [3]. Complex hierarchical structures can be also obtained with independent functionalization of macropore and mesopore networks on the basis of chemical and/or size specificity affords control over the reaction sequence in catalytic cascades [4]. The catalyst preparation strategies also include the addition of other metal oxides to the silica network: in desulfurization process, the prepared mixed oxide would take advantage of both titania, probably as the main active component, and silica, for its high thermal stability, excellent mechanical strength and high surface area [5] and the same approach can be employed for photocatalytic practices [6]. The mixed oxides can also be used as polymerization catalysts, where the presence of oxides such as WO_3, CrO_3 and MoO_3 in the silica network decreased the necessary cocatalyst amount, suggesting that the support nature has a considerable influence on the process [7].

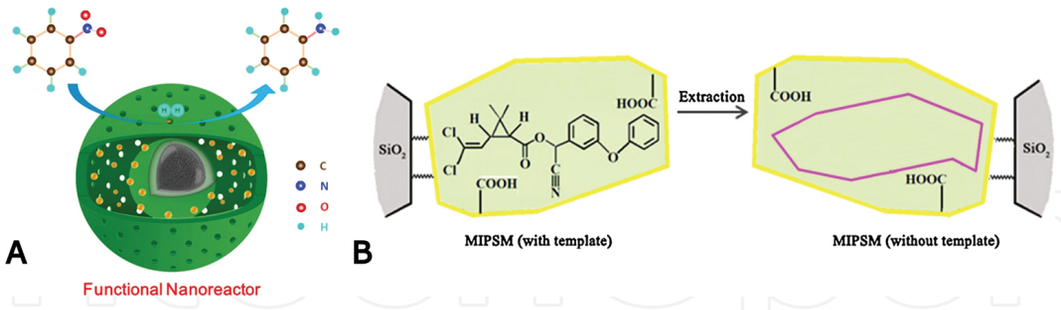

Figure 1. A) Rattle-type magnetic silica composite with nonporous silica-coating magnetic iron oxide encapsulated in mesoporous silica hollow sphere which can also contain active metallic nanoparticles [3]. B) Molecular imprinting process adapted with permission from Zhao et al. [9].

For chromatographic phases and sorbents, the main maneuvers are the so-called molecular imprinting or the silica functionalization with groups that retain the analytes. Taking into consideration the second approach, it is possible to design hybrid silica monoliths functionalized with, for example, aminopropyl or cyanopropyl groups and utilize them as selective stationary phase for microextraction by packed sorbent (MEPS). This method could determine drugs, such as antipsychotics in combination with antidepressants, anticonvulsants and

anxiolytics in plasma samples from schizophrenic patients through liquid chromatography-tandem mass spectrometry (LC-MS/MS) in the multiple reactions monitoring (MRM) mode [8]. On the other hand, the molecular imprinting is a methodology which creates cavities for the analytes encapsulating the analyte itself or a template within the silica network that is followed by an extraction process (**Figure 1B**) [9]. The resulting material is of high specificity, increasing the selectivity and performance of the sorbent/phase. This methodology has been employed to extract important compounds such as the β-N-methylamino-L-alanine amino acid from cyanobacteria which is hypothesized to be linked to amyotrophic lateral sclerosis and Parkinson dementia complex from people living in Guam island [10] and to pretreat, detect and analyze trace levels of toxic pyrethroid insecticides in soils [9].

Different types of sensors can also be prepared taking advantages of silica materials' flexibility. Optical sensors use to employ the methodology of a receptor element encapsulation within the silica network and the structural properties and addition of organic groups can be correlated with the device performance [11]. They frequently include the encapsulation of an organic dye which can change color when in contact with the analyte [12]. The introduction of mixed oxides and organic groups can be of high importance in this field to avoid leaching of these dyes during usage [13]. It is also possible to manufacture different devices' configuration such as nanosensors for pH measurement [13], optical fibers for volatile organic compounds' detection [14], electrochemical [15], electrochemiluminescence [16] and biosensors [17]. Furthermore, silica is commonly used to protect or give special features to surfaces. In terms of protection, organosilanes are well known as corrosion protectors for metallic surfaces such as steel and aluminum alloys [18], where other metal such as cerium [19], metallic nanoparticles such as $NiFe_2O_4$ [20] and other compounds such as phosphonic acid [21] can also be added to the coating to enhance the protection. The surface characteristics are another feature that are able to be tuned by the silica coatings. In this field, it is possible to mention the superhydrophobicity that is widely explored with the possibility of self-cleaning surface creation [22, 23] and also the addition of antimicrobial properties is of high importance [24, 25].

Thus, the chapter shall be structured according to the following subitems:

1. *Introduction on silica-based materials*. A panorama on the different applications of such devices (catalysts, chromatographic phases, sorbents, coatings…) should be provided, illustrating recent examples from the literature (2014–2015). Some comments on the general aspects of their production (synthetic routes based on sol-gel routes, grafting reactions, encapsulation via nonhydrolytic sol-gel processes, molecular imprinting).

2. *Organic groups on silica surface*. Recent examples of the use of FTIR and FT-Raman spectroscopies in the monitoring of surface reactions between silanol groups and ligands for organic and organometallic compounds. The possibility of distinguishing liquid-like and crystalline configuration for long-chain alkyl groups from the C–H stretching vibrations position.

3. *Molecules within bulk silica.* The use of FTIR in monitoring the encapsulation of molecules within silica network by deconvolution of Si–O stretching region. The correlation between siloxane four- or six-membered rings and device characteristics/properties.

4. *Silica molecular imprinting*. The use of FTIR and Raman in the monitoring of cavity interaction between templates/target molecules with functional groups from silica pores.
5. *FTIR and Raman modes*. Discussion on the complementary information provided by sampling accessories and detection modes in the characterization/evaluation of hybrid silica materials, namely: attenuated total reflectance (ATR), DRIFTS, photoacoustic spectroscopy (PAS), infrared emission spectroscopy (IRES), micro-FTIR and Raman.

2. Organic groups on silica surface

Recent examples of the use of FTIR and FT-Raman spectroscopies in the monitoring of surface reactions between silanol groups and ligands for organic and organometallic compounds. The possibility of distinguishing liquid-like and crystalline configuration for long-chain alkyl groups from the C–H stretching vibrations position.

The organic groups' presence and interactions are monitored in different types of materials, as the ones discussed above. In terms of corrosion protection coatings, the organosilanes are widely known that due to their efficient properties as coupling agents, representing an interesting and environmentally friendly alternative in the field of surface treatments [26]. One of the employed organosilanes is the glycidyloxypropyltrimethoxysilane (GPS) that when mixed with methyltriethoxysilane can improve coating resistance, charge transfer resistance and present low-frequency impedance parameters. FTIR was employed by Foroozan et al. [18] to investigate the reaction between glycidyl groups of GPS molecules with silanol groups. It was possible to identify bands reflecting the epoxy ring breathing around ~910 and 840 cm^{-1} and also a new band appeared near 1730 cm^{-1} for C=O stretching that could be associated with the oxidation of the epoxide ring. The spectra confirmed a strong network reticulation as a result of the reaction between glycidyl groups of GPS molecules with hydrolyzed silanes. However, the complimentary results of water contact angles decreased probably due to higher amount of –CH–OH, produced in the reaction between glycidyl and silanol groups, so they reached an optimum point at which a more reticulated structure overcomes the silane layer hydrophilicity.

Silanol groups are also employed to investigate the grafting of catalytic compounds at the silica surface. Ochędzan-Siodłak et al. describes a catalytic system where metallocenes and postmetallocene compounds are immobilized in an ionic liquid modified silica surface. The modification process could be followed by the Si–OH stretching vibration, at 3700 cm^{-1}, disappearing after the ionic liquid modified silane reaction with the silanol groups (**Figure 2A**) [27]. This strategy is becoming popular nowadays, where different organosilanes are first used to modify the surface with specific chemical groups with which is possible to graft the catalysts species or precursors itself [28, 29]. Similarly, the Si–OH vibration can be used to follow direct grafting of catalyst in the silica surface, where the silanol groups can react with a metallic center producing chemical bond between the catalyst compound and the silica surface. Li et al. [30] describes the grafting of a nickel complex in silica and alumina surfaces by following a band at 3745 cm^{-1}, which is assigned to isolated surface hydroxyl groups drops gradually with

reaction time and almost completely vanishes after 24 h and correspondingly the absorption bands at 3070–2877 cm^{-1} related to C–H stretching vibrations of the catalyst allyl groups steadily raise in intensity (**Figure 2B**). Capel-Sanchez et al. [31] also investigated the grafting by silanol groups and in the development of a single site titanium on an amorphous silica surface, they report that the titanium precursor is preferentially anchored over the silica surface by the bridging hydroxyl groups (broad band around 3500 and 3700 cm^{-1}) over the isolated ones (~3700 cm^{-1}).

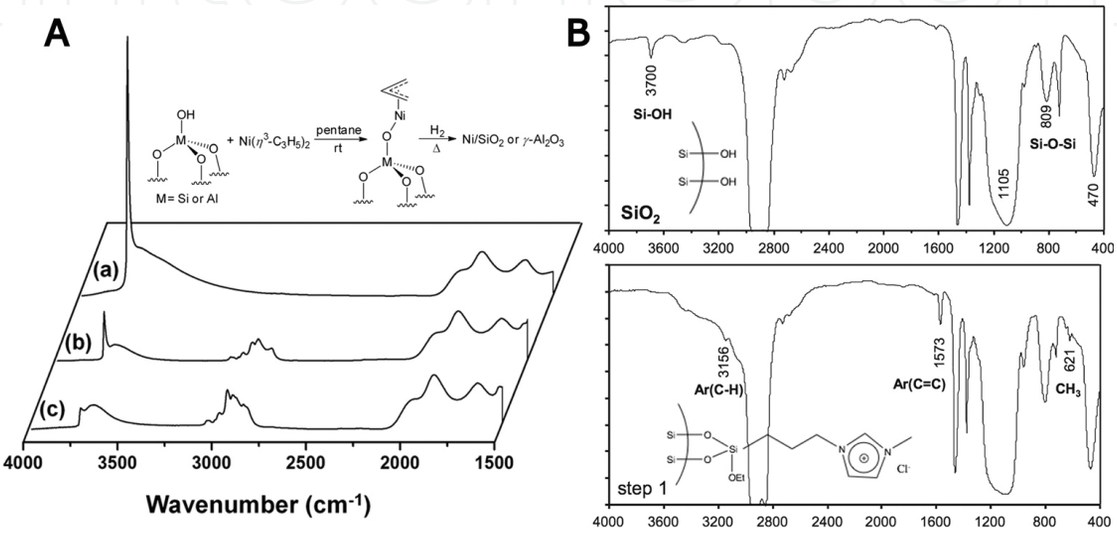

Figure 2. Monitoring of Si–OH stretching vibration, at 3700 cm^{-1}, disappearing after (A) the grafting of a nickel complex in silica and alumina surfaces [27] and (B) the ionic liquid modified silane reaction with the silanol groups [30].

By using Raman spectroscopy, there is also the possibility of final conformation studies in the case of hybrid silica with long alkyl chains at the silica surface. Structure and order information about alkane-based systems can be obtained from multiple indicators in their Raman spectra, especially in the ν(C–H) region between 2750 and 3050 cm^{-1}. Also, significant conformational order information exists for alkane systems in the ν(C–C) and δ(C–H) regions between 900 and 1500 cm^{-1}. However, it is necessary some care about fluorescence phenomena interferences in Raman around this region [32]. Using this methodology, Brambilla et al. evaluated the gauche and trans conformation of hybrid silica with different octadecyl groups (octadecylsilane [ODS]) content by Raman spectroscopy. The two bands centered at 1080 and 1062 cm^{-1} are assigned, respectively, to *ν*(C–C) for *gauche* e *trans* conformation of the ODS alkyl chains. The ratio in intensity of these two bands was evaluated in order to monitor the influence of the TEOS/ODS molar ratio in the organic groups' behavior. For all ratios, the intensity between the two bands laid above 1, meaning there is a predominance of *trans* conformation in comparison to *gauche* one, indicating therefore an intense molecular organization in the hybrid silica prepared by the sol-gel method. In addition, it was found that the organization degree of alkyl chains decreases with the ODS content increase, with data from 29Si-NMR and FTIR detected in attenuated total reflectance (ATR) mode, corroborating to the findings [33].

3. Molecules within bulk silica

The FTIR technique can also be employed to evaluate silica network characteristics such as hydrophilicity/hydrophobicity degree and siloxane ring structure regarding thin film porosity [34, 35]. In terms of sensors, these features may impact the analyte interaction and access to the encapsulated molecules, known as receptor elements, within the silica matrix. If the encapsulated molecules' interaction with the silica network occurs through their active sites, it is possible that these active sites are not available to further interact with the analyte. Reduced sensor performance can also occur if the silica network is nonpermeable. In this case, the silica network itself limits the pathways the analyte can travel to reach the encapsulated receptor molecules hindering the reaction. Consequently, both cases could reduce the sensor performance or completely disable it [36].

Silica materials have a prominent band corresponding to the Si–O–Si bond asymmetric stretching in the region from 1300 to 1000 cm^{-1}. Literature reports that the maximum centers and relative intensities of the longitudinal optic (LO) and transversal optic (TO) modes of this bond are shifted with the introduction of chemical groups or organic molecules in the silica network [35]. So, a complete analysis of its components can be conducted, including the deconvolution of the LO and TO modes in their relative main contributions: the four-membered $(SiO)_4$ and six-membered $(SiO)_6$ siloxane rings (**Figure 3A**), resulting in a total of four components (LO_6, LO_4, TO_6 and TO_4) (**Figure 3B**). Usually, materials with higher content of chemical groups or organic molecules use to present higher formation of less stressed six-membered ring, thereby allowing a better accommodation of the nonreactive organic groups [37]. Furthermore, there is a correlation between the formation of six-membered rings and an increase in the relative degree of crystallinity, as well as with the long-range organization in hybrid silica materials that is normally observed with an increase in the degree of matrix alkylation [38].

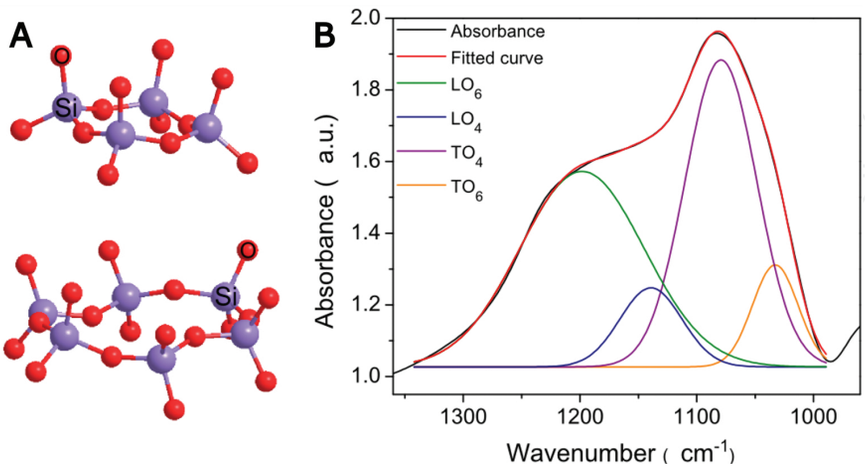

Figure 3. A) Two of the most common cyclical arrangements of SiO_4 structural units in xerogels: four-membered siloxane ring $(SiO)_4$ above and six-membered siloxane ring $(SiO)_6$ below. B) Band deconvolution to asymmetric stretching ν(Si–O(–Si)) bond [39].

http://dx.doi.org/10.5772/64477

Using this approach, a series of silica-based acid-base optical sensors prepared by encapsulating pH indicators using three different sol-gel routes was investigated [36]. The employed routes were: nonhydrolytic, acid-catalyzed and base-catalyzed and the pH indicators were alizarin red, brilliant yellow and acridine. The FTIR spectra were performed for all the materials and the peak corresponding to the Si–O–Si asymmetric stretching was deconvoluted and their respective components analyzed and **Figure 4** assembles the results. For the acidic and nonhydrolytic routes, a positive correlation between the pH indicator content and the increase in $(SiO)_6$ percentage was established, thereby indicating the silica network structure rearrangement in order to accommodate the indicator molecules. Using a basic route, the reached indicator contents were notably low and so this relationship was not observed. In addition, no relationship between the $(SiO)_6$ percentage and the response time could be established in spite of less dense networks, with bigger rings, might render easier the analyte permeation. This behavior may indicate that the analyte probably accessed the receptor elements through the passages between the siloxane rings and not through the siloxane rings themselves [36].

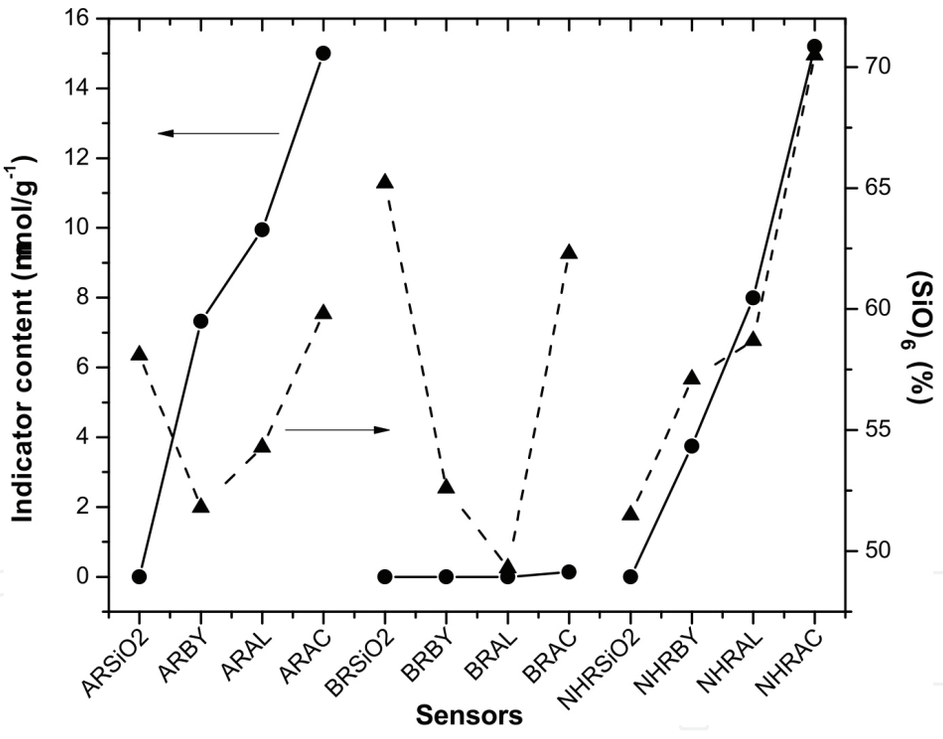

Figure 4. Comparison of $(SiO)_6$ percentage () and encapsulated indicator content () in each sample [39].

It is remarkable that depending on the sol-gel route, the rate between hydrolysis and condensation reactions will change with the pH medium and can explain the behavior of the basic-catalyzed sensor material. Under basic conditions, the condensation reactions of silanol groups are strongly accelerated, and the particles are rapidly formed. Thus, the probability of rearrangement as a function of the presence of other molecules, as pH indicators for example, during the synthesis decreases, since the tridimensional network is quickly formed. When the

condensation reactions are slower, such occurs in acid pH, the network can be more influenced by the addition of molecules to be encapsulated [39].

4. Silica molecular imprinting

The molecular imprinting methodology involves a molecular recognition process where the analyte can recognize and preferentially bind to specific sites built by using a template of the target molecule during the matrix network formation. After an extraction process in order to remove the template, the resulting material is bulk silica with cavities that are morphologically and stereochemically compatible with the analyte. Therefore, an option of analytical technique to follow this procedure is FTIR. It is possible to track the template interaction with the silica network by the template bands appearance and/or SiO_2 vibrations change.

With this approach, Morais et al. [40] describe the interactions of different drugs such as fluoxetine, gentamicin, lidocaine, morphine, nifedipine, paracetamol and tetracycline with silica matrix during the preparation of molecular imprinting materials. All these drugs present nitrogen atoms as primary, secondary or tertiary amines that can interact with silanol groups. The investigation was performed comparing the vibrations of bare drug with the encapsulated drug, before removal by extraction. The silica spectrum presents intense bands in the region of ~3500 cm^{-1} assigned to the O–H vibrations of silanol groups and adsorbed water; and in the region of 1200–800 cm^{-1}, where the Si–O stretchings are observed. As a result of these strong bands and the frequently low concentrations of the encapsulated compounds, it is common to observe an overlapping of their signals by the silica ones avoiding this type of evaluation [36].

As an example, **Figure 5A** illustrates the spectra of lidocaine with its main bands at 1675 cm^{-1} is assigned to the ν(C=O) of the amide chemical group, 1655 and 1546 cm^{-1} attributed to δ(C–N–H) of the amine group and the band at 1476 cm^{-1} to the δ(C–CH_3) of the methyl group; and **Figure 5B** shows the spectra of the lidocaine-silica composite where the main bands of the drug can still be observed. However, the bands assigned to the carbonyl stretching and amino bending modes were shifted to 1683 and 1639 cm^{-1}, respectively, suggesting a potential medicine-silica network interaction through these chemical groups. Similar behavior was observed for the other drugs, considering the machine resolution of 4 cm^{-1}. Most of the pharmaceutical presented infrared band shifts toward higher wave numbers (bathochromic shift) when encapsulated, indicating they are interacting with the silica structure, resulting in a rearrangement of the chemical groups, which was confirmed by the rotational isomerism of the molecule. In addition, some of the bands were shifted for lower wave numbers (hypsochromic shift) reflecting a tension increase in the molecule rotational conformation, since the encapsulation process may incur in difficulty of the functional groups vibrational movements demanding more energy. Most of the nitrogen-related bands, for all samples, had their wave numbers shifted. These results denote possibility of a hydrogen bonding interaction through electron donation between these groups and silica network, as illustrated by **Figure 6**. Among the studied drugs, the exception was tetracycline which presented a shift in the OH group deformation band and so indicating an interaction by this group [40].

http://dx.doi.org/10.5772/64477

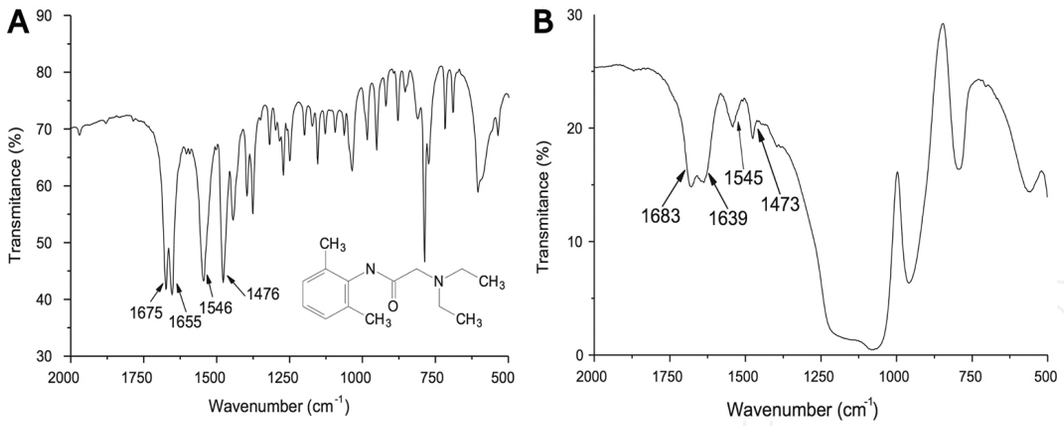

Figure 5. FTIR spectra of bare lidocaine (A) and the respective encapsulated system (B) [40].

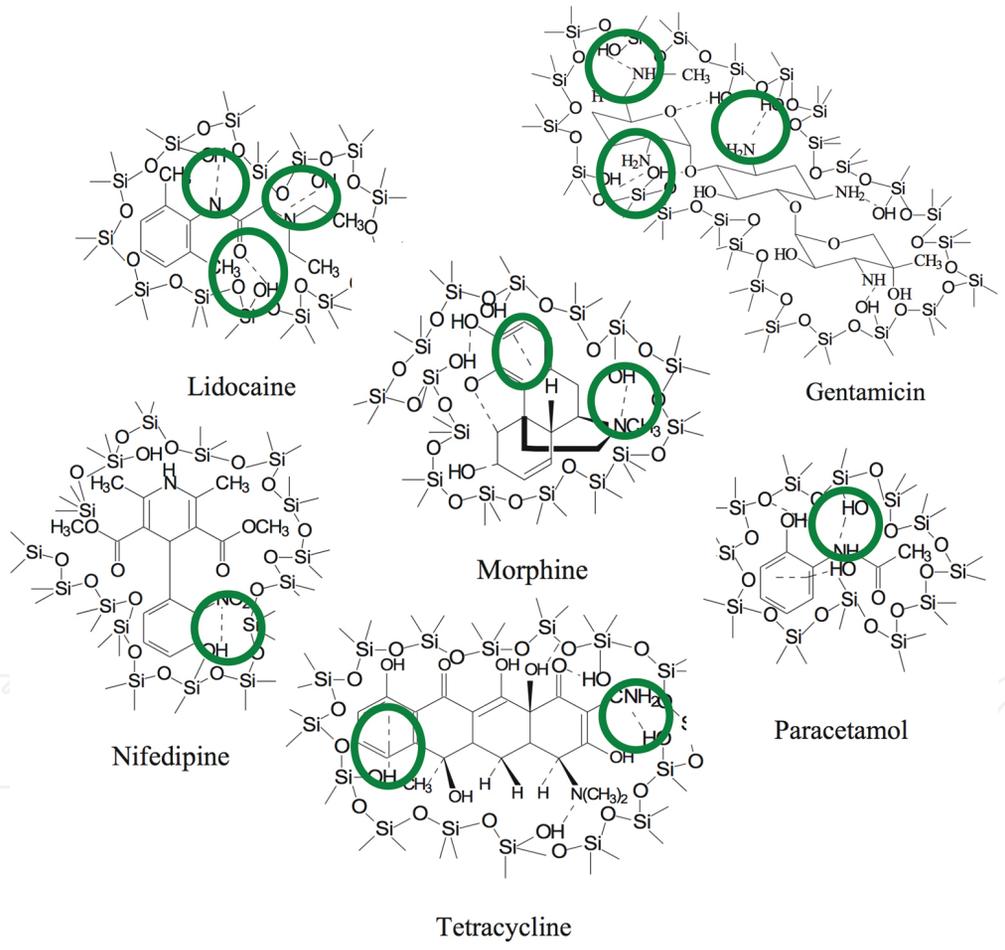

Figure 6. Proposed interactions of the drugs with silica network [40].

In other approaches, hybrid silica networks have been used to improve both the process of molecular imprinting as the following usage of the material as an extraction matrix. Han et al. reports the functionalization of silica with amino groups provided by aminopropyltriethoxy-

silane to help interaction with the toxic herbicide pentachlorophenol [41]. By using FTIR to monitor this process, they were able to identify the N–H bond around 1560 cm^{-1} and C–H bond around 2935 cm^{-1}, suggesting the $–NH_2$ grafting onto the activated silica gel surface. In this case, imprinted and nonimprinted sorbents showed similar location and appearance of the major bands, reflecting the already mentioned problem of overlapping bands with the major bands of silica network. Similar behavior was observed by Chrzanowska et al., Ren et al. and Li et al. [42–44]. The first one employed the functionalization of silica nanoparticles surface with aminopropyl groups to promote the encapsulation of biochanin A, producing a selective solid-phase extraction of biochanin A, daidzein and genistein from urine samples [42]. Analogously, Ren et al. employed the same procedure with aminopropyl groups, although the target analyte was bisphenol A [44]. Finally, the later one made use of propylthiocyanate groups to modify the silica surface, creating a selective phase for selective removal of cadmium(II) competing with copper, zinc and lead in aqueous solution [43]. In all the cases, the assisting organic groups' bands were detected; however, the molecular imprinted and nonimprinted spectra were really similar.

5. FTIR and Raman modes

When analyzing hybrid silica materials, sometimes it is necessary to use complementary techniques to better evaluate the materials' characteristics. The same occurs for vibrational spectroscopy methods. A wide investigation was performed with a series of different hybrid silica prepared with tetraethoxysilane (C_0), methyltriethoxysilane (C_1), octyltriethoxysilane (C_8), octadecyltrimethoxysilane (C_{18}), vinyltrimethoxysilane (Vy), phenyltrimethoxysilane (Ph), mercaptopropyltrimethoxysilane (SHp), isocyanatepropyltriethoxysilane (NCOp), chloropropyltrimethoxysilane (Clp) and glycidoxypropyltrimethoxysilane (Gp) [45]. Using FTIR, the main bands of silica were well determined for all the hybrid silicas and they showed shifts depending on the organic group presenting at the network, although the organic groups' bands were barely seen. Using Raman spectroscopy, the organic groups were well described and some of the silica network bands were also observed.

The region around 3600–3000 cm^{-1} is attributed to hydroxyl groups ν(O–H) stretching modes. The shoulder at ~3600 cm^{-1} matches the OAH vibrations associated with alcohols that are a subproduct of sol-gel reaction, while the maximum at ~3425 cm^{-1} is related to surface –OH participating of hydrogen bonds. Water is also described here as a shoulder at ~3230 cm^{-1}, which is also observed at ~1630 cm^{-1}. As mentioned before, silica presents a characteristic region of peaks from 1250 to 700 cm^{-1} that can provide structural characteristics of the network. Specially, when related to the main bands between 1250 and 1000 cm^{-1} corresponding to the asymmetric ν(Si–O–H) and their deconvolution on LO at ~1130 cm^{-1} and TO at 1047 cm^{-1} modes. The Si–O(H) bond stretching appears at slightly different positions in the FTIR (~950 cm^{-1}) and Raman (~980 cm^{-1}) spectra. The symmetric mode of ν(Si–O–Si) band is found at ~791 (FTIR) and ~799 cm^{-1} (Raman), while the $Si–O^-$ rocking mode was observed at ~540 cm^{-1} (IR). Finally, the Raman spectra also show the siloxane ring breathing mode (with 3 or 4 SiO units) located at ~490 cm^{-1} [45].

The silica-related bands presented wave number shifts depending on the employed organic group in the different hybrid silicas. For Si–O(–Si) LO mode, the largest shift occurs from the nonhybrid to the hybrid samples. In this case, shifts to lower wave numbers use to be related to the network deformation in order to accommodate the organic groups within the inorganic silica matrix resulting in larger siloxane rings and greater Si–O–Si angles and longer Si–O bond lengths. LO and TO mode shifts occur mainly near the surface of the material, which can be better detected employing attenuated total reflectance (ATR) mode of FTIR spectroscopy. In addition, the organic groups' introduction can originate from heterogeneous regions that may introduce local deformations in the network resulting in the differences observed for Si–O bond lengths and Si–O–Si angles in the different hybrid materials. Another interesting behavior is reported to Si–O(H) band, considering that, in a general way for this case, the wave number shifts result from hydrogen bond formation with the silanol groups. A significantly higher wave number occurred for C_{18} while the lower ones occurred for Clp and Gp [45]. The very hydrophobic C_{18} organic chain can hinder hydrogen bond formation by comparison with the other samples, thus, the Si–O bond length is decreased and the wave number is shifted to higher values. However, the groups Clp and Gp can facilitate hydrogen bond formation with the silanol groups and, as a consequence, the Si–O bond length is increased and the vibrational wave number is decreased [46].

As mentioned before, the characterization of the organic groups of hybrid network is better done using Raman spectroscopy than FTIR. The last one can observe only some bands, while Raman presents a series of them showing the complementarity of both techniques for hybrid materials' characterization. **Table 1** compiles some important assignments regarding the organic groups and their respective wave numbers detected by both techniques, when applicable [45].

The complementary use of FTIR and Raman spectroscopies can be also employed to deeply investigate the processes taking place during sol-gel process and there are other types of detection modes for these vibrational techniques as DRIFTS, PAS, IRES, micro-FTIR and Raman which can help.

DRIFT spectroscopy is primarily used on samples where most of the reflected radiation is diffused. It is important that the specular reflectance is reduced to a minimum because it distorts the DRIFT spectrum and lowers the band intensities [47]. During the last years, it has become the most effective technique for studying the processes taking place at the gas-solid interface [48]. Ivanovski et al. investigated the region of the OH stretching vibrations of silica gel activated at different temperatures for the purpose of checking the availability of the OH groups for further reaction with 3-aminopropyltrimethoxysilane (APTMS) molecules and whether chemisorption was successful, finding evidence whether chemisorption of APTMS involves all available methoxy groups. It is also possible to investigate the conformation of the aminopropyl groups (APS) backbone on the silica gel surface and the possible proton transfer between the NH_2 groups of APS and OH from silica gel detected by the formation of NH_3^+ and SiO^- which is spectroscopically detectable through the appearance of the $\delta(NH_3^+)$ vibrations at 1668 cm^{-1} [49]. In addition, Bukleski et al. developed a direct quantitative method of quantification of maximal chemisorption of 3-aminopropylsilyl groups on silica gel using

DRIFT spectroscopy, as (APS) modified silica gel plays an important role as a precursor for further modifications, where APS acts as a spacer or bridging molecule. By integrating the spectra in the frequency range of the $\nu(CH_2)/\nu(CH_3)$ vibrations between 3014 and 2808 cm^{-1}, the mass fraction of APTMS of 19.04% was found to correspond to a maximal concentration of APS on silica gel of 2.23 μmol m^{-2}, which was confirmed by elemental analysis for carbon [47].

Assignment	C1	C8	C18	Vy	Ph	SHp	NCOp	Clp	Gp
$C–H_{(3)\ asym}$	2979 R	2955 I	2957 I						
$C–H_{(3)\ sym}$	2916 R	2884 R	2883 R						
$C–H_{(2)\ asym}$		2932 R	2930 R			2928 R	2939 R	2962 R	2926 R
		2926 I	2918 I			2942 I	2945 I	2960 I	2935 I
$C–H_{(2)\ sym}$		2861 R	2850 R			2894 R	2897 R	2901 R	2894 R
		2856 I	2848 I						2880 I
$C–H_{\ arom}$					3058 R				
Si–C	1412 R				1122 R				
	1280 I								
$CH_{2\ bend}$		1463 R	1460 R						
		1457 I	1468 I						
C–C		1064 R	1062 R	1013 R	999 R				
C=C				1603 R					
$=C–H_{\ term}$				3072 R					
$=C–H_{\ term\ bend}$				1412 R					
				1278 R					
(Si)C–H				2991 R					
$C–H_{\ bend}$					1432 i				
$Ring_{\ breath}$					737 I				1260 R
$Ring_{\ def}$					698 I				
S–H						2574 R			
C–S						652 R			
C=N							1553 I		
N=C=O							1449 R		
$H–C–Cl_{\ def}$								1412 R	
$C–Cl(H)_{trans}$								645 R	
OC–H									1456 R

*asym: asymmetric; sym: symmetric; bend: bending; term: terminal; def: deformation; R: Raman; and I: infrared.

Table 1. Organic group bands detected by the complementary techniques of FTIR and Raman [45].

The photoacoustic spectroscopy (PAS) FTIR is a broad-applicable mid-infrared solution when samples present opacity problems [50]. It is a unique extension of IR spectroscopy which combines the utility of interferometry with the standard sample-gas microphone of the photothermal technique for depth-profile analysis of materials. Its signal generation processes automatically and reproducibly isolates a layer extending beneath the sample surface which has suitable optical density for analysis without physically altering the sample. PAS involves measurement of acoustic wave (pressure oscillations) in a hermetically sealed cell fitted with a very sensitive microphone. The microphone signal, when plotted as a function of wavelength, contains a spectrum proportional to the absorption spectrum of the sample. The wave generation follows absorption of light, which is modulated at a frequency in the acoustic range, by the sample. Most FTIR instruments provide modulation frequencies between 50 and 500 Hz in the 400–4000 cm^{-1} wave number span [51]. Therefore, this approach can be employed to evaluate silica samples as described by Gao et al. to widely explore a polyethylene-*co*-Zn-acrylic acid hybrid material prepared by the sol-gel process. They could identify both vibrations for silica and the organic group. By investigating the silica bands it is noted that not only silica but also other forms of silicon groups are formed via the sol-gel reaction, while the existence of the Si–OH group indicates that the condensation reaction was not completely finished. However, analyzing the peaks referring to the organic groups, it was reported that $–CH_2–$ and $–CH_3$ positions in the region of 2800–3000 cm^{-1} remain the same after hybrid material fabrication, indicating no chemical bond between silicon and these two groups forms after the sol-gel reaction. The band at 1700 cm^{-1} is the C=O stretching mode from the –COOH group was also noticed for both materials. This is due to unneutralized acrylic acid. While the transparency of the hybrid is a result of strong organic-inorganic interaction, and a high degree of mixing, no evidence of hydrogen bonding is observed from the FTIR peak position [52].

Infrared emission spectroscopy (IRES) is a method in which a sample is energized by heating and so on, and the infrared light emitted from the sample is measured to obtain a spectrum. It utilizes the contrast between the sample and the base material with possibility of an improved signal-to-noise ratio compared to absorption spectroscopy. Ideally only photons emitted by the sample are detected ("zero background"), free from the noise produced by the continuum lamp in an absorption experiment. This improvement in sensitivity is particularly useful for the spectroscopy of transient molecules because of their intrinsically low concentrations [53]. In the case of hybrid silicas, this methodology can be successfully employed to evaluate the thermal stability of materials. Brambilla et al., for example, describe the behavior of octadecylsilane (ODS) hybrid silicas prepared by grafting and sol-gel methods with a spectra series from 100 to 900°C between 4000 and 500 cm^{-1}. The decrease of physically adsorbed water band and the surface silanol interactions, leading to an increase in the band at 3747 cm^{-1}, attributed to isolated silanol groups was observed. For temperatures higher than 450°C up to 900°C, the band assigned to isolated silanol groups (3747 cm^{-1}) is reduced due to condensation reactions and structural reorganization with generation of siloxane groups. Concerning the ν(C–H) stretching region, the bands at 2963, 2929 and 2855 cm^{-1} are reduced in the range of 250–550°C, as a result of the thermal degradation of ODS chains. **Figure 7** presents the relative band area for this vibration. It was possible to compare the thermal stability of hybrid materials

prepared by grafting (GR100) and sol-gel method (SG10A), confirm the higher thermal stability of the first one [54].

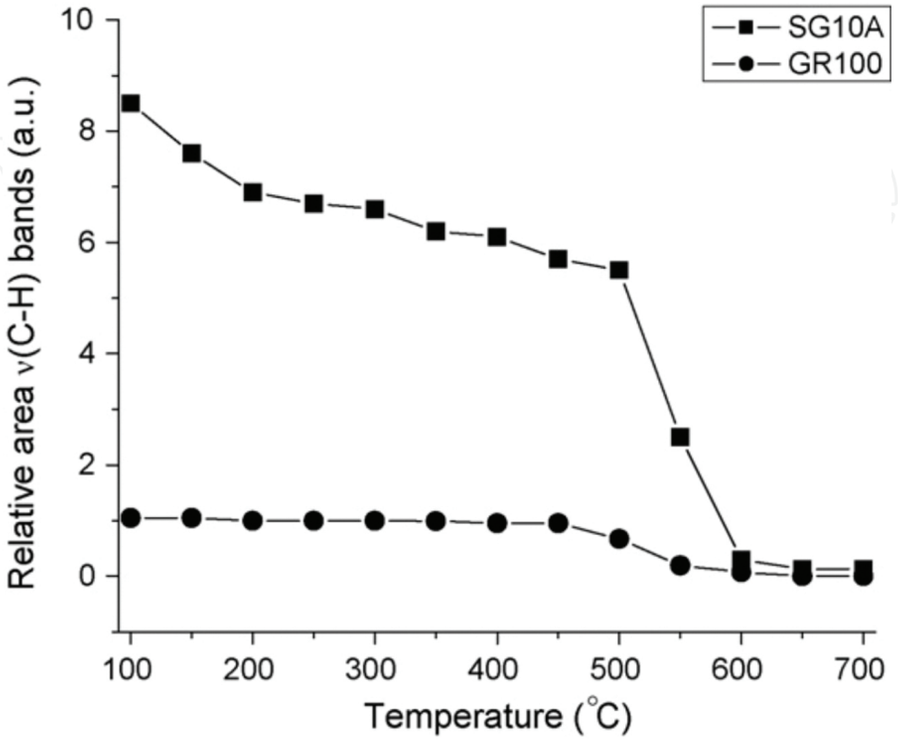

Figure 7. Relative area of ν(C–H) bands versus temperature for grafting prepared (GR100) and sol-gel prepared (SG10) hybrid silicas [54].

Finally, micro-Raman and micro-FTIR modes have less sensibility, however, they are key methods employed when spatial resolution of a few micrometers is necessary. It can be employed, for example, to evaluate radial distribution of the fictive temperature in pure silica optical fibers [55], porous silica supports for individual living cells [56] and phenyl-bridged polysilsesquioxane positive and negative resist for electron beam lithography where the technique helped to propose a description of the tone switching mechanisms [57].

6. Final remarks

Observing all the procedures and results described above, it is noticeable that a vibrational spectrum is not collected only to simply evaluate peak positions anymore. Nowadays, it is possible to obtain deep information about materials' formation, evolution and structure, as well as to acquire spatial resolution spectra or in high-resolution modes with low signal/noise ratios. The reaction chemical processes following methods are getting more and more specific, as collected data are more and more exploited in order to give the maximum results information, bringing fast advance in the materials characterization field.

Author details

Larissa Brentano Capeletti and João Henrique Zimnoch*

*Address all correspondence to: jhzds@iq.ufrgs.br

Chemistry Institute, Federal University of Rio Grande do Sul, Porto Alegre, Brazil

References

[1] M. Perchacz, H. Benes, L. Kobera, Z. Walterova, Influence of sol–gel conditions on the final structure of silica-based precursors. Journal of Sol-Gel Science and Technology, 75 (2015) 649–663. DOI: 10.1007/s10971-015-3735-z.

[2] T.Y. Amiri, J. Moghaddas, Cogeled Copper-Silica Aerogel as a Catalyst in Hydrogen Production from Methanol Steam Reforming. International Journal of Hydrogen Energy, 40 (2015) 1472–1480. DOI: 10.1016/j.ijhydene.2014.11.104.

[3] C.Z. Jin, Y.J. Wang, H.L. Tang, K.X. Zhu, X. Liu, J.H. Wang, Versatile Rattle-Type Magnetic Mesoporous Silica Spheres, Working as Adsorbents and Nanocatalyst Containers. Journal of Sol-Gel Science and Technology, 77 (2016) 279–287. DOI: 10.1007/s10971-015-3830-1.

[4] C.M.A. Parlett, M.A. Isaacs, S.K. Beaumont, L.M. Bingham, N.S. Hondow, K. Wilson, A.F. Lee, Spatially Orthogonal Chemical Functionalization of a Hierarchical Pore Network for Catalytic Cascade Reactions. Nature Materials, 15 (2016) 178–182. DOI: 10.1038/nmat4478.

[5] A. Bazyari, A.A. Khodadadi, A.H. Mamaghani, J. Beheshtian, L.T. Thompson, Y. Mortazavi, Microporous Titania-Silica Nanocomposite Catalyst-Adsorbent for Ultra-Deep Oxidative Desulfurization. Applied Catalysis B – Environmental, 180 (2016) 65–77. DOI: 10.1016/j.apcatb.2015.06.011.

[6] B. Moongraksathum, Y.W. Chen, Preparation and Characterization of SiO2-TiO2 Neutral Sol by Peroxo Sol–gel Method and Its Application on Photocatalytic Degradation. Journal of Sol-Gel Science and Technology, 77 (2016) 288–297. DOI: 10.1007/s10971-015-3853-7.

[7] A.A. Bernardes, C. Radtke, M.D.M. Alves, I.M. Baibich, M. Lucchese, J.H.Z. dos Santos, Synthesis and Characterization of SiO2-CrO3, SiO2-MoO3, and SiO2-WO3 Mixed Oxides Produced Using the Non-Hydrolytic Sol–gel Process. Journal of Sol-Gel Science and Technology, 69 (2014) 72–84. DOI: 10.1007/s10971-013-3188-1.

[8] I.D. de Souza, D.S. Domingues, M.E.C. Queiroz, Hybrid Silica Monolith for Microextraction by Packed Sorbent to Determine Drugs from Plasma Samples by Liquid

Chromatography-Tandem Mass Spectrometry. Talanta, 140 (2015) 166–175. DOI: 10.1016/j.talanta.2015.03.032.

[9] M.Y. Zhao, X.D. Ma, F.J. Zhao, H.W. Guo, Molecularly Imprinted Polymer Silica Monolith for the Selective Extraction of Alpha-Cypermethrin from Soil Samples. Journal of Materials Science, 51 (2016) 3440–3447. DOI: 10.1007/s10853-015-9661-1.

[10] P. Svoboda, A. Combes, J. Petit, L. Novakova, V. Pichon, B. Grp, Synthesis of a Molecularly Imprinted Sorbent for Selective Solid-Phase Extraction of Beta-N-Methylamino-L-Alanine. Talanta, 144 (2015) 1021–1029. DOI: 10.1016/j.talanta.2015.07.052.

[11] S. Islam, N. Bidin, S. Riaz, S. Naseem, F.M. Marsin, Correlation between Structural and Optical Properties of Surfactant Assisted Sol–Gel Based Mesoporous SiO2-TiO2 Hybrid Nanoparticles for pH Sensing/Optochemical Sensor. Sensors and Actuators B – Chemical, 225 (2016) 66–73. DOI: 10.1016/j.snb.2015.11.016.

[12] P.C.A. Jeronimo, A.N. Araujo, M. Montenegro. Optical Sensors and Biosensors Based on Sol–gel Films. Talanta, 72 (2007) 13–27.

[13] S. Islam, N. Bidin, S. Riaz, G. Krishnan, S. Naseem, Sol–Gel Based Fiber Optic pH Nanosensor: Structural and Sensing Properties. Sensors and Actuators A – Physical, 238 (2016) 8–18. DOI: 10.1016/j.sna.2015.12.003.

[14] J.C. Echeverria, M. Faustini, J.J. Garrido, Effects of the Porous Texture and Surface Chemistry of Silica Xerogels on the Sensitivity of Fiber-Optic Sensors toward VOCS. Sensors and Actuators B – Chemical, 222 (2016) 1166–1174. DOI: 10.1016/j.snb.2015.08.010.

[15] E.M. Caldas, E.W. de Menezes, T.M. Pizzolato, S.L.P. Dias, T.M.H. Costa, L.T. Arenas, E.V. Benvenutti, Ionic Silsesquioxane Film Immobilized on Silica Applied in the Development of Carbon Paste Electrode for Determination of Methyl Parathion. Journal of Sol-Gel Science and Technology, 72 (2014) 282–289. DOI: 10.1007/s10971-014-3367-8.

[16] A.M. Spehar-Deleze, S. Almadaghi, C.K. O'Sullivan, Development of Solid-State Electrochemiluminescence (ECL) Sensor Based on Ru(bpy)(3)(2+)-Encapsulated Silica Nanoparticles for the Detection of Biogenic Polyamines. Chemosensors, 3 (2015) 178–189. DOI: 10.3390/chemosensors3020178.

[17] A.R. Mukhametshina, S.V. Fedorenko, I.V. Zueva, K.A. Petrov, P. Masson, I.R. Nizameev, A.R. Mustafina, O.G. Sinyashin, Luminescent Silica Nanoparticles for Sensing Acetylcholinesterase-Catalyzed Hydrolysis of Acetylcholine. Biosensors & Bioelectronics, 77 (2016) 871–878. DOI: 10.1016/j.bios.2015.10.059.

[18] A. Foroozan, R. Naderi, Effect of Coating Composition on the Anticorrosion Performance of a Silane Sol–Gel Layer on Mild Steel. RSC Advances, 5 (2015) 106485–106491. DOI: 10.1039/c5ra21744j.

[19] I. Santana, A. Pepe, E. Jimenez-Pique, S. Pellice, I. Milosev, S. Cere, Corrosion Protection of Carbon Steel by Silica-Based Hybrid Coatings Containing Cerium Salts: Effect of

Silica Nanoparticle Content. Surface & Coatings Technology, 265 (2015) 106–116. DOI: 10.1016/j.surfcoat.2015.01.050.

[20] M. Gharagozlou, R. Naderi, Z. Baradaran, Effect of Synthesized NiFe2O4-Silica Nanocomposite on the Performance of an Ecofriendly Silane Sol–gel Coating. Progress in Organic Coatings, 90 (2016) 407–413. DOI: 10.1016/j.porgcoat.2015.08.009.

[21] V. Dalmoro, J.H.Z. dos Santos, L.M. Baibich, I.S. Butler, E. Armelin, C. Aleman, D.S. Azambuja, Improving the Corrosion Performance of Hybrid Sol–Gel Matrix by Modification with Phosphonic Acid. Progress in Organic Coatings, 80 (2015) 49–58. DOI: 10.1016/j.porgcoat.2014.11.018.

[22] S.A. Mahadik, F. Pedraza, R.S. Vhatkar, Silica Based Superhydrophobic Coating for Long-Term Industrial and Domestic Applications. Journal of Alloys and Compounds, 663 (2016) 487–493. DOI: 10.1016/j.jallcom.2015.12.016.

[23] A.C. Power, A. Barrett, J. Abubakar, L.J. Suarez, L. Ryan, D. Wencel, T. Sullivan, F. Regan, Versatile Self-Cleaning Coating Production through Sol–gel Chemistry. Advanced Engineering Materials, 18 (2016) 76–82. DOI: 10.1002/adem.201500112.

[24] R. Arreche, N. Bellotti, M. Blanco, P. Vazquez, Improved Antimicrobial Activity of Silica-Cu Using a Heteropolyacid and Different Precursors by Sol–Gel: Synthesis and Characterization. Journal of Sol-Gel Science and Technology, 75 (2015) 374–382. DOI: 10.1007/s10971-015-3710-8.

[25] W.L. Storm, J.A. Johnson, B.V. Worley, D.L. Slomberg, M.H. Schoenfisch, Dual Action Antimicrobial Surfaces Via Combined Nitric Oxide and Silver Release. Journal of Biomedical Materials Research, Part A, 103 (2015) 1974–1984. DOI: 10.1002/jbm.a.35331.

[26] M. Fedel, E. Callone, S. Dire, F. Deflorian, M.G. Olivier, M. Poelman, Effect of Na-Montmorillonite Sonication on the Protective Properties of Hybrid Silica Coatings. Electrochimica Acta, 124 (2014) 90–99. DOI: 10.1016/j.electacta.2013.11.006.

[27] W. Ochedzan-Siodlak, K. Dziubek, Metallocenes and Post-Metallocenes Immobilized on Ionic Liquid-Modified Silica as Catalysts for Polymerization of Ethylene. Applied Catalysis A – General, 484 (2014) 134–141. DOI: 10.1016/j.apcata.2014.07.016.

[28] S. Ray, P. Das, A. Bhaumik, A. Dutta, C. Mukhopadhyay, Covalently Anchored Organic Carboxylic Acid on Porous Silica Nano Particle: A Novel Organometallic Catalyst (PSNP-Ca) for the Chromatography-Free Highly Product Selective Synthesis of Tetrasubstituted Imidazoles. Applied Catalysis A – General, 458 (2013) 183–195. DOI: 10.1016/j.apcata.2013.03.024.

[29] M.S. Saraiva, C.I. Fernandes, T.G. Nunes, C.D. Nunes, M.J. Calhorda, New MO(II) Complexes in MCM-41 and Silica: Synthesis and Catalysis. Journal of Organometallic Chemistry, 751 (2014) 443–452. DOI: 10.1016/j.jorganchem.2013.07.081.

[30] L.D. Li, E. Abou-Hamad, D.H. Anjum, L. Zhou, P.V. Laveille, L. Emsley, J.M. Basset, Well-Defined Mono(Eta(3)-Allyl)Nickel Complex MoNi(Eta(3)-C3H5) (M = Si or Al)

Grafted onto Silica or Alumina: A Molecularly Dispersed Nickel Precursor for Syntheses of Supported Small Size Nickel Nanoparticles. Chemical Communications, 50 (2014) 7716–7719. DOI: 10.1039/c4cc02962c.

[31] M.C. Capel-Sanchez, G. Blanco-Brieva, J.M. Campos-Martin, M.P. de Frutos, W. Wen, J.A. Rodriguez, J.L.G. Fierro, Grafting Strategy to Develop Single Site Titanium on an Amorphous Silica Surface. Langmuir, 25 (2009) 7148–7155. DOI: 10.1021/la900578u.

[32] C.J. Orendorff, J.E. Pemberton, Raman Spectroscopic Study of the Conformational Order of Octadecylsilane Stationary Phases: Effects of Electrolyte and pH. Analytical and Bioanalytical Chemistry, 382 (2005) 691–697. DOI: 10.1007/s00216-005-3133-4.

[33] R. Brambilla, G.P. Pires, N.P. da Silveira, J.H.Z. dos Santos, M.S.L. Miranda, R.L. Frost, Spherical and Lamellar Octadecylsilane Hybrid Silicas. Journal of Non-Crystalline Solids, 354 (2008) 5033–5040. DOI: 10.1016/j.jnoncrysol.2008.07.031.

[34] R.M. Almeida, T.A. Guiton, C.G. Pantano, Detection of LO Mode in V-SiO2 by Infrared Diffuse Reflectance Spectroscopy. Journal of Non-Crystalline Solids, 119 (1990) 238–241 DOI: 10.1016/0022-3093(90)90847-f.

[35] A. Fidalgo, L.M. Ilharco, Chemical Tailoring of Porous Silica Xerogels: Local Structure by Vibrational Spectroscopy. Chemistry – A European Journal, 10 (2004) 392–398. DOI: 10.1002/chem.200305079.

[36] L.B. Cappeletti, E. Moncada, J. Poisson, I.S. Butler, J.H.Z. Dos Santos, Determination of the Network Structure of Sensor Materials Prepared by Three Different Sol–gel Routes Using Fourier Transform Infrared Spectroscopy (FT-IR). Applied Spectroscopy, 67 (2013) 441–447. DOI: 10.1366/12-06748.

[37] A. Fidalgo, R. Ciriminna, L.M. Ilharco, M. Pagliaro, Role of the Alkyl-Alkoxide Precursor on the Structure and Catalytic Properties of Hybrid Sol–gel Catalysts. Chemistry of Materials, 17 (2005) 6686–6694. DOI: 10.1021/cm051954x.

[38] S.L.B. Lana, A.B. Seddon, X-Ray Diffraction Studies of Sol–Gel Derived Ormosils Based on Combinations of Tetramethoxysilane and Trimethoxysilane. Journal of Sol-Gel Science and Technology, 13 (1998) 461–466. DOI: 10.1023/a:1008685614559.

[39] L.B. Capeletti, J.H.Z. Dos Santos, E. Moncada, Dual-Target Sensors: The Effect of the Encapsulation Route on pH Measurements and Ammonia Monitoring. Journal of Sol-Gel Science and Technology, 64 (2012) 209–218. DOI: 10.1007/s10971-012-2849-9.

[40] E.C. Morais, G.G. Correa, R. Brambilla, C. Radtke, I.M. Baibich, J.H.Z. dos Santos, The Interaction of Encapsulated Pharmaceutical Drugs with a Silica Matrix. Colloids and Surfaces B – Biointerfaces, 103 (2013) 422–429. DOI: 10.1016/j.colsurfb.2012.10.059.

[41] D.M. Han, G.Z. Fang, X.P. Yan, Preparation and Evaluation of a Molecularly Imprinted Sol–gel Material for On-Line Solid-Phase Extraction Coupled with High Performance

Liquid Chromatography for the Determination of Trace Pentachlorophenol in Water Samples. Journal of Chromatography A, 1100 (2005) 131–136. DOI: 10.1016/j.chroma.2005.09.035.

[42] A.M. Chrzanowska, A. Poliwoda, P.P. Wieczorek, Surface Molecularly Imprinted Silica for Selective Solid-Phase Extraction of Biochanin A, Daidzein and Genistein from Urine Samples. Journal of Chromatography A, 1392 (2015) 1–9. DOI: 10.1016/j.chroma.2015.03.015.

[43] Z.C. Li, H.T. Fan, Y. Zhang, M.X. Chen, Z.Y. Yu, X.Q. Cao, T. Sun, Cd(II)-Imprinted Polymer Sorbents Prepared by Combination of Surface Imprinting Technique with Hydrothermal Assisted Sol–Gel Process for Selective Removal of Cadmium(II) from Aqueous Solution. Chemical Engineering Journal, 171 (2011) 703–710. DOI: 10.1016/j.cej.2011.05.023.

[44] Y.M. Ren, W.Q. Ma, J. Ma, Q. Wen, J. Wang, F.B. Zhao, Synthesis and Properties of Bisphenol A Molecular Imprinted Particle for Selective Recognition of BPA from Water. Journal of Colloid and Interface Science, 367 (2012) 355–361. DOI: 10.1016/j.jcis.2011.10.009.

[45] L.B. Capeletti, I.M. Baibich, I.S. Butler, J.H.Z. dos Santos, Infrared and Raman Spectroscopic Characterization of Some Organic Substituted Hybrid Silicas. Spectrochimica Acta Part A – Molecular and Biomolecular Spectroscopy, 133 (2014) 619–625. DOI: 10.1016/j.saa.2014.05.072.

[46] A. Fidalgo, L.M. Ilharco, The Defect Structure of Sol–gel-Derived Silica/Polytetrahydrofuran Hybrid Films by FTIR. Journal of Non-Crystalline Solids, 283 (2001) 144–154. DOI: 10.1016/s0022-3093(01)00418-5.

[47] M. Bukleski, V. Ivanovski, E. Hey-Hawkins, A Direct Method of Quantification of Maximal Chemisorption of 3-Aminopropylsilyl Groups on Silica Gel Using Drift Spectroscopy. Spectrochimica Acta Part A – Molecular and Biomolecular Spectroscopy, 149 (2015) 69–74. DOI: 10.1016/j.saa.2015.04.026.

[48] N. Tasinato, D. Moro, P. Stoppa, A.P. Charmet, P. Toninello, S. Giorgianni, Adsorption of F2C=CFCL on TiO2 Nano-Powder: Structures, Energetics and Vibrational Properties from Drift Spectroscopy and Periodic Quantum Chemical Calculations. Applied Surface Science, 353 (2015) 986–994. DOI: 10.1016/j.apsusc.2015.07.006.

[49] V. Ivanovski, M. Bukleski, M. Madalska, E. Hey-Hawkins, Vibrational Spectra of a Ferrocenyl Phosphine Derivative Chemisorbed on 3-Aminopropylsilyl Modified Silica Gel. Vibrational Spectroscopy, 69 (2013) 57–64. DOI: 10.1016/j.vibspec.2013.09.009.

[50] J.F. McClelland, R.W. Jones, S. Luo, L.M. Seaverson, A Practical Guide to FTIR Photoacoustic Spectroscopy, In: P.B. Coleman (Ed.) Practical Sampling Techniques for Infrared Analysis, CRC Press, Boca Raton, 1993, pp. 320.

[51] R. Kizil, J. Irudayaraj, Fourier Transform Infrared Photoacoustic Spectroscopy (FTIR-PAS), In: G.C.K. Roberts (Ed.) Encyclopedia of Biophysics, Springer Berlin Heidelberg, Berlin, Heidelberg, 2013, pp. 840–844.

[52] Y. Gao, N.R. Choudhury, N. Dutta, J. Matisons, M. Reading, L. Delmotte, Organic–inorganic Hybrid from Ionomer Via Sol–gel Reaction. Chemistry of Materials, 13 (2001) 3644–3652. DOI: 10.1021/cm010179s.

[53] P.F. Bernath, 6 Infrared Emission Spectroscopy. Annual Reports Section "C" (Physical Chemistry), 96 (2000) 177–224. DOI: 10.1039/B001200I.

[54] R. Brambilla, J.H.Z. dos Santos, M.S.L. Miranda, R.L. Frost, Thermal Stability of Octadecylsilane Hybrid Silicas Prepared by Grafting and Sol–gel Methods. Thermochimica Acta, 469 (2008) 91–97. DOI: 10.1016/j.tca.2008.01.010.

[55] C. Martinet, V. Martinez, C. Coussa, B. Champagnon, M. Tomozawa, Radial Distribution of the Fictive Temperature in Pure Silica Optical Fibers by Micro-Raman Spectroscopy. Journal of Applied Physics, 103 (2008) 4. DOI: 10.1063/1.2905321.

[56] O. Cristini-Robbe, K. Raulin, F. Dubart, R. Bernard, C. Kinowski, N. Damene, I. El Yazidi, A. Boed, S. Turrell, Porous Silica Supports for Micro-Raman Spectroscopic Studies of Individual Living Cells. Journal of Molecular Structure, 1050 (2013) 232–237. DOI: 10.1016/j.molstruc.2013.06.063.

[57] L. Brigo, V. Auzelyte, K.A. Lister, J. Brugger, G. Brusatin, Phenyl-Bridged Polysilsesquioxane Positive and Negative Resist for Electron Beam Lithography. Nanotechnology, 23 (2012) 7. DOI: 10.1088/0957-4484/23/32/325302.